Journal of Organometallic Chemistry, 406 (1991) 219–236
Elsevier Sequoia S.A., Lausanne
JOM 21412

Reactions of some triosmium clusters of the type $Os_3(\mu\text{-}H)_2(CO)_9Ar$ ($Ar = C_6H_4$, C_9H_6, C_4H_3N, or C_4H_2NMe) with phosphines and phosphites; X-ray crystal structure of $Os_3(\mu\text{-}H)_2(CO)_7[P(OMe)_3]_2(C_4H_3N)$

Hong Chen, Brian F.G. Johnson, Jack Lewis * and Paul R. Raithby
University Chemical Laboratory, Lensfield Road, Cambridge CB2 1EW (UK)

(Received September 4th, 1990)

Abstract

Triosmium clusters with the formulation $Os_3(\mu\text{-}H)_2(CO)_9Ar$ [$Ar = C_6H_4$ (**1**), C_9H_6 (**2**), C_4H_3N (**3**), or C_4H_2NMe (**4**)] can be chemically activated by reaction with Me_3NO/MeCN to produce the reactive species $Os_3(\mu\text{-}H)_2(CO)_{9-n}(MeCN)_nAr$ [$n = 1$, $Ar = C_6H_4$ (**5**), C_9H_6 (**6**), C_4H_3N (**7**), or C_4H_2NMe (**8**); $n = 2$, $Ar = C_6H_4$ (**9**), C_9H_6 (**10**), C_4H_3N (**11**), or C_4H_2NMe (**12**)], which then react with phosphine or phosphite molecules to give substituted products $Os_3(\mu\text{-}H)_2(CO)_{9-n}(PR_3)_nAr$ ($n = 1$, or 2, R = Ph, Et, or OMe). These clusters have been characterised by spectroscopic techniques, and $Os_3(\mu\text{-}H)_2(CO)_7[P(OMe)_3]_2(C_4H_3N)$ (**24**) has been structurally characterised by an X-ray analysis. In this complex one of the phosphite ligand occupies an axial site on the osmium triangle while the second occupies a more conventional equatorial site. The C_4H_3N ligand caps the triangle and is coordinated through the nitrogen and one carbon atom.

Introduction

Osmium and ruthenium clusters containing the μ_3-*o*-phenylene ligand, C_6H_4, are readily obtained from the oxidative addition reaction of $M_3(CO)_{12}$ (M = Os, Ru) with arylphosphines or arylarsines, or the thermolysis of clusters containing these ligands, via P–C or As–C and C–H bond cleavage and M–C and M–H bond formation [1–8]. The benzyne cluster $Os_3(\mu\text{-}H)_2(CO)_9(C_6H_4)$ (**1**) has been prepared from the direct reaction of $Os_3(CO)_{12}$ with benzene in low yield [9], and can also be obtained from the photolysis of $Os_3(CO)_9(\eta^6\text{-}C_6H_6)$ [10]. The activated cluster $Os_3(CO)_{10}(MeCN)_2$ reacts with a series of arenes to give clusters of the type of $Os_3(\mu\text{-}H)_2(CO)_9(C_6H_2R^1R^2)$ [11]. The crystal structure of (**1**) (Fig. 1) [11] shows that the benzyne ligand lies over one face of the metal triangle, forming two σ-bonds and one π-bond to the osmium atoms, a bonding mode found for many alkyne and alkene complexes [12]. This bonding mode is adopted by most of the benzyne species reported, while some adopt a slightly different bonding mode [5,7,13], where the benzyne ligand is bound asymmetrically to the bent chain of three osmium

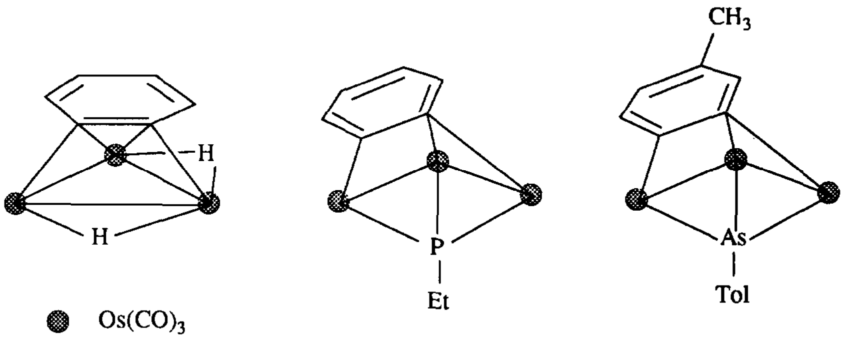

$H_2Os_3(CO)_9(C_6H_4)$ (**1**) $Os_3(CO)_9(C_6H_4)(PEt_3)$ $Os_3(CO)_9(C_6H_3Me)(AsTol)$

Fig. 1. Structures of some benzyne clusters.

atoms with one carbon atom linked to one metal atom and the adjacent atom bound to the other two metal atoms (Fig. 1).

We are interested in some analogues of $Os_3(\mu\text{-}H)_2(CO)_9(C_6H_4)$ (**1**), i.e. $Os_3(\mu\text{-}H)_2(CO)_9(C_9H_6)$ (**2**) [14], $Os_3(\mu\text{-}H)_2(CO)_9(C_4H_3N)$ (**3**) [15] and $Os_3(\mu\text{-}H)_2(CO)_9(C_4H_2NMe)$ (**4**) [16] because of their close structural relation to **1** in that they have very similar IR spectra in the CO stretching region and the organic ligands adopt the same bonding mode as in the benzyne complexes (Fig. 2).

Although the studies of fluxionality of benzyne and related species have been carried out [13,17–19], the chemistry of these clusters have not been studied in detail [20]. While the reaction of $Os_3(\mu\text{-}H)_2(CO)_9(C_6H_4)$ (**1**) with diphenylacetylene [21] and the Friedel–Crafts reactions on the organic moieties of clusters **1**–**4** [22] have been reported previously, here we wish to report the substitution reaction of complexes **1**–**4** with phosphine and phosphite ligands, and analyse the diversity of isomers found in the products.

Results and discussion

Clusters **1**–**4** are readily activated by reaction with Me_3NO/MeCN to yield mono- and bis-acetonitrile derivatives **5**–**12** (Scheme 1), which display similar IR spectra to (Table 1). These complexes are highly reactive and air-sensitive, and have

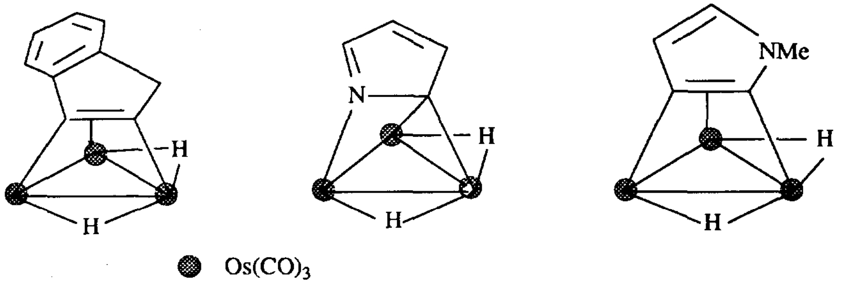

$H_2Os_3(CO)_9(C_9H_6)$ (**2**) $H_2Os_3(CO)_9(C_4H_3N)$ (**3**) $H_2Os_3(CO)_9(C_4H_2NMe)$ (**4**)

Fig. 2. Structures of clusters 2–4.

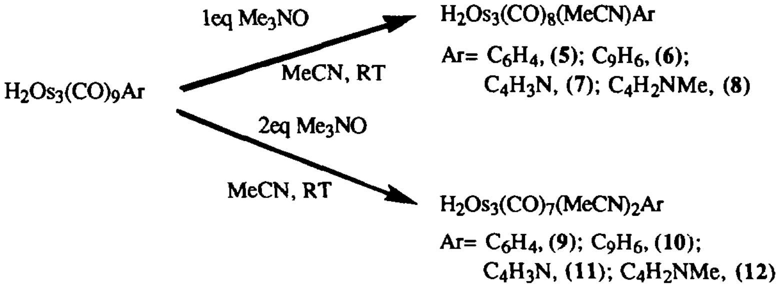

Scheme 1. Activation of **1**–**4** by $Me_3NO/MeCN$.

not been isolated. The acetonitrile ligand(s) in these clusters are easily displaced by phosphine and phosphite ligands.

(i) Reactions of $H_2Os_3(CO)_8(MeCN)(C_6H_4)$ *(5) and* $H_2Os_3(CO)_7(MeCN)_2(C_6H_4)$ *(9) with* PR_3 *(R = Ph, OMe)*

Clusters **5** and **9** react with PPh_3 or $P(OMe)_3$, in CH_2Cl_2, at room temperature to form $Os_3(\mu\text{-}H)_2(CO)_8(PR_3)(C_6H_4)$ [R = Ph (**13**); OMe (**14**)] and $Os_3(\mu\text{-}H)_2(CO)_7(PR_3)_2(C_6H_4)$ [R = Ph (**15**); OMe (**16**)], respectively. Clusters **13**–**15** have also been synthesised from the photolysis of the face capping benzene clusters $Os_3(CO)_{9-n}(PR_3)_n(\mu_3\text{-}\eta^2:\eta^2:\eta^2\text{-}C_6H_6)$ [10] (R = Ph, $n = 1$, or 2; R = OMe, $n = 1$) (Scheme 2).

Clusters **13** and **14** have been studied exhaustively by NMR [10] and have been shown to have two isomeric forms. Possible structures for the isomers are shown in Fig. 3.

In the case of PPh_3 substitution, the PPh_3 ligand in the major isomer appears to occupy an axial site, while for $P(OMe)_3$ substitution the ligand in the major isomer occupies an equatorial site. This feature may reflect the difference in steric requirements of the two types of phosphorus donor ligands since the steric repulsion between C_6H_4 moiety and the bulky PPh_3 ligand could be minimised with the PPh_3 occupying the axial position.

While the bis-triphenylphosphine substituted cluster $Os_3(\mu\text{-}H)_2(CO)_7(PPh_3)_2(C_6H_4)$ (**15**) has only one isomer, which might adopt the structure shown in Fig. 4 which is consistent with ^1H NMR studies [22], the trimethylphosphite analogue

Table 1

IR spectra of clusters **5**–**12**

Compound	IR (ν(CO), cm^{-1}, in MeCN)
$H_2Os_3(CO)_8(MeCN)(C_6H_4)$ (**5**)	2081w, 2046vs, 2035s,sh, 1993s, 1971m.
$H_2Os_3(CO)_8(MeCN)(C_9H_6)$ (**6**)	2081w, 2046s, 2036ms, 1996m, 1971m.
$H_2Os_3(CO)_8(MeCN)(C_4H_3N)$ (**7**)	2081w, 2046vs, 2036m, 1996m, 1971m.
$H_2Os_3(CO)_8(MeCN)(C_4H_2NMe)$ (**8**)	2076m, 2041vs, 2025s, 1991s, 1976s.
$H_2Os_3(CO)_7(MeCN)_2(C_6H_4)$ (**9**)	2057w, 2025m, 1989s, 1973m, 1961m, 1941vw.
$H_2Os_3(CO)_7(MeCN)_2(C_9H_6)$ (**10**)	2057w, 2025m, 1989s, 1974m, 1958m.
$H_2Os_3(CO)_7(MeCN)_2(C_4H_3N)$ (**11**)	2056w, 2025s, 1987s, 1972s, 1919vw
$H_2Os_3(CO)_7(MeCN)_2(C_4H_2NMe)$ (**12**)	2056w, 2019m, 1978s, 1953m, 1911vw.

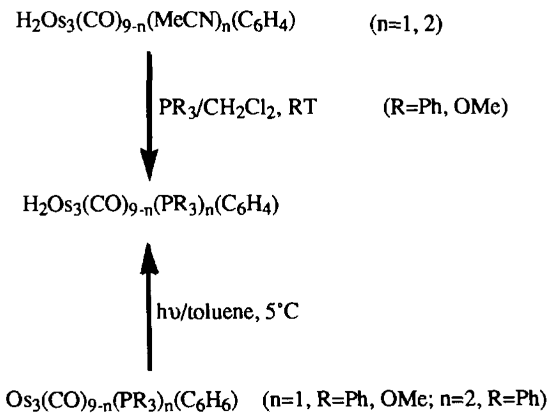

Scheme 2. Synthetic routes to clusters **13–16**.

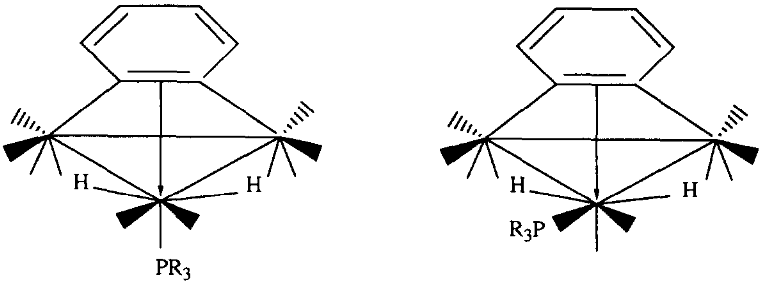

R= Ph	(13a)		R= Ph	(13b)
2		:	1	
OMe	(14a)		OMe	(14b)
1		:	9	

Fig. 3. Proposed structures for **13** and **14**.

$Os_3(\mu\text{-}H)_2(CO)_7[P(OMe)_3]_2(C_6H_4)$ (**16**) has two isomers. The ^1H NMR spectrum of **16** at room temperature shows broad resonances, while in that at 190 K the resonances for two isomers are observed. The major isomer (**16a**) has two apparent doublets (δ 7.76, 7.62) and two apparent triplets (δ 6.78, 6.58) for the C_6H_4 group, implying that the molecule is asymmetric. The ^1H NMR data indicates that one

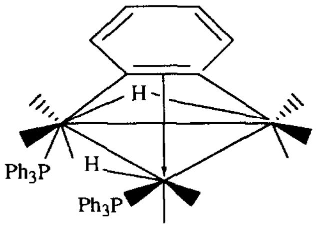

Fig. 4. Proposed structure for **15**.

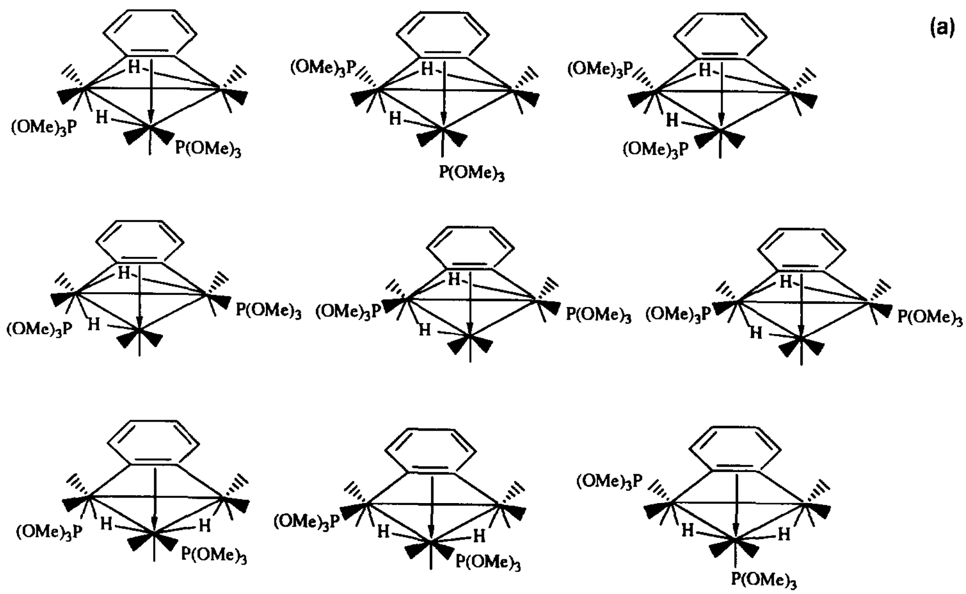

Fig. 5a. Possible structures for the major isomer **16a**.

hydride ligand is *trans* to one phosphite ligand (J(PH) = 44 Hz) and *cis* to the other (J(PH) = 9.3 Hz). The second hydride is *cis* to only one of the phosphite ligands (J(PH) = 14.8 Hz). Thus, the possible structures of the major isomer are postulated as in Fig. 5a. For the minor isomer, only P(OMe)$_3$ and the hydride

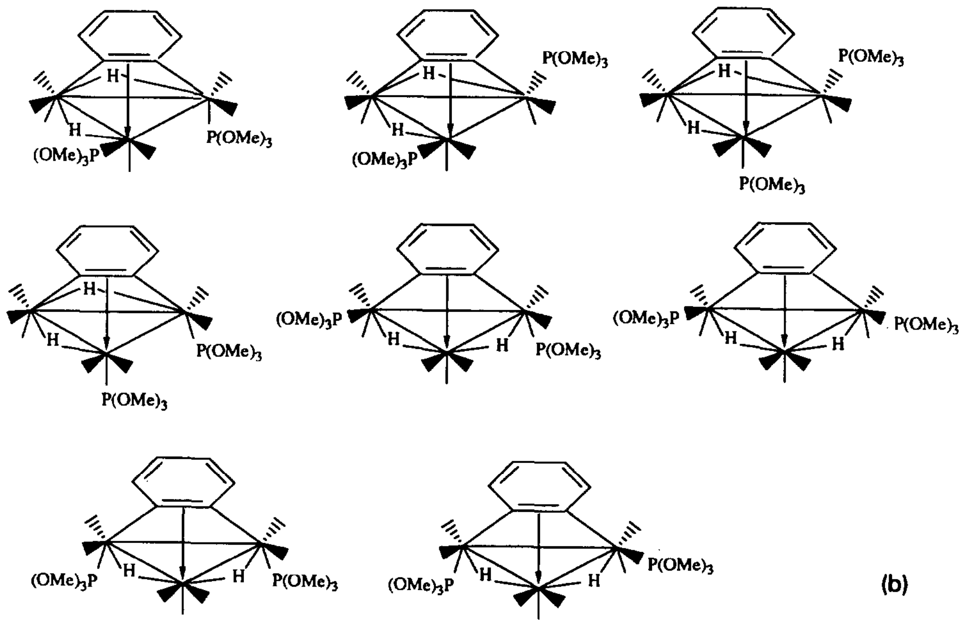

Fig. 5b. Possible structures for the minor isomer **16b**.

$Os_3(\mu\text{-}H)_2(CO)_{9-n}(MeCN)_n(C_9H_6)$ (n=1,2)

$$\Big\downarrow \; PR_3 \text{ or } P(OR)_3/CH_2Cl_2/\Delta$$

$Os_3(\mu\text{-}H)_2(CO)_{9-n}(PR_3)_n(C_9H_6)$ (n=1,2)

or

$Os_3(\mu\text{-}H)_2(CO)_{9-n}(P(OR)_3)(C_9H_6)$ (n=1,2)

R=Me, Et

Scheme 3. Synthetic routes to clusters **17**–**20**.

resonances are identified, while the benzene signals are not resolved. Both hydride ligands appear as doublets (J(PH) = 15.0 and 14.9 Hz, respectively) in the ^{1}H NMR spectrum suggesting both coupling to only one phosphite ligand in a *cis*-position (Fig. 5b).

(ii) Reactions of $Os_3(\mu\text{-}H)_2(CO)_8(MeCN)(C_9H_6)$ (6) and $Os_3(\mu\text{-}H)_2(CO)_7(MeCN)_2$-$(C_9H_6)$ (10) with PR_3 (R = Et, or OMe)

Clusters **6** and **10** react smoothly with phosphine and phosphite ligands in dichloromethane at room temperature or under reflux to give substituted products **17**–**20** (Scheme 3). Better yields are obtained under refluxing condition.

Clusters **17**–**20** were also characterised spectroscopically, and again, the hydride region of their ^{1}H NMR spectra is very useful for the elucidation of their structures. The complex $Os_3(\mu\text{-}H)_2(CO)_8(PEt_3)(C_9H_6)$ (**17**) has been shown to have two isomers in the ratio of 2 : 1 and in both cases the phosphine ligand is probably *cis* to one hydride ligand (J(PH) = 12 Hz) and *trans* to the other (J(PH) = 18 Hz) (Fig. 6).

In both isomers **17a** and **17b**, the PEt_3 ligand occupies an equatorial position, which is different from that observed for the benzyne clusters **13** and **14**. In the latter case, phosphine or phosphite ligand occupies an equatorial site to give an asymmetrical isomer or takes an axial position to give a symmetrical isomer (Fig. 3), while in the case of (**17**), the occupation of different equatorial sites by PEt_3 ligand results in two isomers due to the asymmetry of the molecule.

The phosphite analogue, $Os_3(\mu\text{-}H)_2(CO)_8[P(OMe)_3](C_9H_6)$ (**18**) also exists in different isomeric forms as evidenced by the ^{1}H NMR spectrum. The major isomer probably adopts a similar structure to that of **17**, but the minor isomer is almost undetectable because its proton resonances are very weak and unresolved. For both the complexes $Os_3(\mu\text{-}H)_2(CO)_7(PEt_3)_2(C_9H_6)$ (**19**) and $Os_3(\mu\text{-}H)_2(CO)_7$-$[P(OMe)_3]_2(C_9H_6)$ (**20**) the hydride signals are not well-resolved, and it is therefore difficult to propose their structures.

(iii) Reactions of $Os_3(\mu\text{-}H)_2(CO)_8(MeCN)(C_4H_3N)$ (7) and $Os_3(\mu\text{-}H)_2CO)_7$-$(MeCN)_2(C_4H_3N)$ (11) with PR_3 (R = Et, or OMe)

The reaction of $Os_3(\mu\text{-}H)_2(CO)_8(MeCN)(C_4H_3N)$ (**7**) with PEt_3 in CH_2Cl_2 at room temperature gives $Os_3(\mu\text{-}H)_2(CO)_8(PEt_3)(C_4H_3N)$ (**21**) which from the ^{1}H

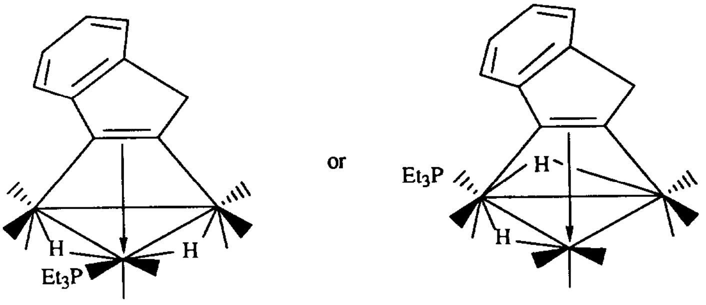

(17a)

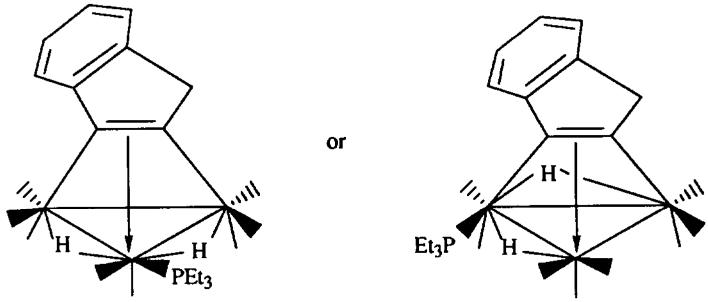

(17b)

Fig. 6. Proposed structures for the two isomers of $Os_3(\mu\text{-}H)_2(CO)_8(PEt_3)(C_9H_6)$ (**17**).

NMR data gives only one isomer, while the reaction with $P(OMe)_3$ leads to two isomers of $Os_3(\mu\text{-}H)_2(CO)_8[P(OMe)_3](C_4H_3N)$ (**22a** and **22b**). The data for **21** are consistent with the PEt_3 ligand occupying an equatorial site where it is *cis* to one hydride (J(PH) = 12.3 Hz) and *trans* to the other (J(PH) = 22.0 Hz) (Fig. 7a). The major isomer of $Os_3(\mu\text{-}H)_2(CO)_8[P(OMe)_3](C_4H_3N)$ (**22a**) has a very large *trans* $^{31}P-^{1}H$ coupling (ca. 51 Hz) and a *cis* $^{31}P-^{1}H$ coupling (13.3 Hz). It is therefore likely to have a structure similar to that of **21**, while the $P(OMe)_3$ ligand in the minor isomer might be in the axial position to give *cis* coupling to both hydride ligands (Fig. 7b).

The reaction of $Os_3(\mu\text{-}H)_2(CO)_7(MeCN)_2(C_4H_3N)$ (**11**) with PEt_3 and $P(OMe)_3$ gives only one isomer in each case, and the ^{1}H NMR spectra of $Os_3(\mu\text{-}H)_2(CO)_7(PEt_3)_2(C_4H_3N)$ (**23**) and $Os_3(\mu\text{-}H)_2(CO)_7[P(OMe)_3]_2(C_4H_3N)$ (**24**) suggest structures in which either both phosphine or phosphite ligands occupy axial positions, or that one is in an axial position while the other is in an equatorial site to give one doublet and one triplet in the hydride region with *cis* $^{31}P-^{1}H$ coupling (Fig. 8).

It is quite interesting that from the reaction of **11** and $P(OMe)_3$, a compound formulated as $Os_3(\mu\text{-}H)_2(CO)_7(MeCN)[P(OMe)_3](C_4H_3N)$ (**25**) is isolated. Although its molecular ion is not observed in the mass spectrum, ^{1}H NMR spectrum shows unambiguously the resonance for one $P(OMe)_3$ ligand at δ 3.69 (d, J(PH) = 12.0 Hz), and that for an acetonitrile group, a singlet at δ 2.52. The phosphite ligand has a two-bond *cis*-coupling (J(PH) = 12.0 Hz) with one hydride and a

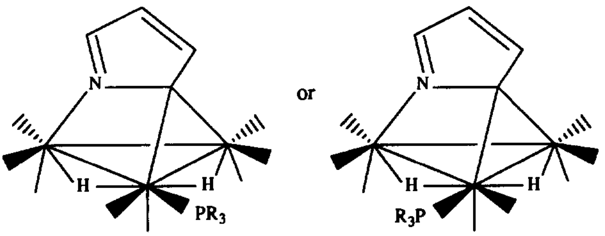

Fig. 7a. Proposed structures for **21** (R = Et) and **22a** (R = OMe).

three-bond coupling (J(PH) = 3.0 Hz) with the other. It is difficult to formulate the structure of **25** since the phosphite ligand and the acetonitrile ligand could have different positions with respect to each other.

*(iv) Crystal structure determination of $Os_3(\mu\text{-}H)_2(CO)_7[P(OMe)_3]_2(C_4H_3N)$ (**24**)*

In order to confirm the spectroscopic assignments and to establish the positions of the phosphite ligands an X-ray diffraction study of **24** was undertaken since the suitable crystals were available. Yellow platelets of $Os_3(\mu\text{-}H)_2(CO)_7[P(OMe)_3]_2(C_4H_3N)$ (**24**) were grown from CH_2Cl_2/hexane solution at −5 °C. The molecular structure of **24** is shown in Fig. 9, with bond lengths listed in Table 2 and bond angles in Table 3.

The crystal structure of **24** consists of discrete molecules of $Os_3(\mu\text{-}H)_2(CO)_7[P(OMe)_3]_2(C_4H_3N)$ separated by normal Van der Waals's distances. The metal framework in **24** is best described as an irregular triangle of Os atoms. The pyrrole, C_4N ring is planar and lies perpendicular to the Os_3 plane (dihedral angle 90.5(5)°). The pyrrole nitrogen, N(1), is bound to Os(3) while C(7) bridges the Os(1)–Os(2) edge, in a manner similar to that observed in the parent complex, $Os_3(\mu\text{-}H)_2(CO)_9(C_4H_3N)$ [23]. An attempt was also made to refine the structure with the positions of N(1) and C(7) reversed, but this lead to a larger R factor, larger thermal parameters on nitrogen and a contraction of those for carbon, as would be expected if the nitrogen and carbon positions were interchanged. One phosphite group occupies an axial site on Os(1) *pseudo-trans* to C(7) [P(1)–Os(1)–C(7), 171.1(4)°] while the second phosphite takes up a more conventional equatorial site on Os(3). The seven carbonyl ligands are essentially linear and occupy terminal sites on the osmium framework; Os(1) has two carbonyls, both equatorial, and Os(2) has three, one axial and two equatorial, and Os(3) has two, one axial and one equatorial. The two bridging hydrides were not located directly but potential energy

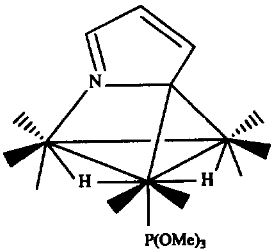

Fig. 7b. Proposed structure for the minor isomer (**22b**).

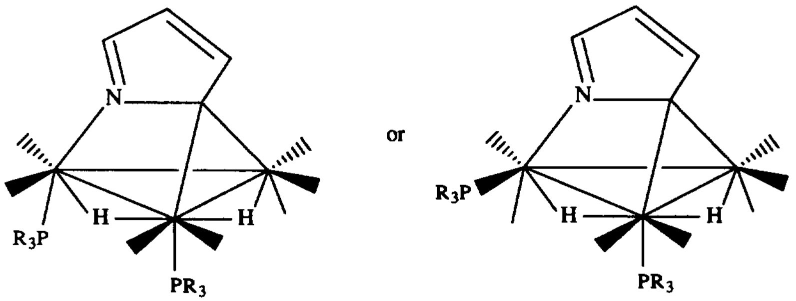

Fig. 8. Possible structures for **23** (R = Et) and **24** (R = OMe).

calculations [24] indicate that they bridge the Os(1)–Os(2) and Os(1)–Os(3) edges, in a configuration similar to that found in $Os_3(\mu\text{-}H)_2(CO)_9(C_4H_3N)$ [23].

The Os–Os distances in the Os triangle of **24** lie within the normal range [11] for such interactions and follow the same trends as observed in the related cluster $Os_3(\mu\text{-}H)_2(CO)_9(C_4H_3N)$ [23]. The presence of the edge-bridging hydrides causes the lengthening of the Os–Os edges while the capping C_4H_3N ligand has an edge shortening influence, particularly on the dibridged Os(1)–Os(2) edge.

The Os(3)–N(1), the Os(1)–C(7), and the Os(2)–C(7) distances in **24** are similar to those found in $Os_3(\mu\text{-}H)_2(CO)_9(C_4H_3N)$ [23], while the same slight asymmetry in the Os–C distances, the N–C and C–C bond lengths within the ring also follow the same trends as in the unsubstituted cluster, with the short N(1)–C(10) [1.319(19) Å] and C(8)–C(9) [1.313(22) Å] indicating multiple bond character. However, the N(1)–C(7) and C(7)–C(8) lengths of 1.401(17) and 1.435(20) Å, respectively, involv-

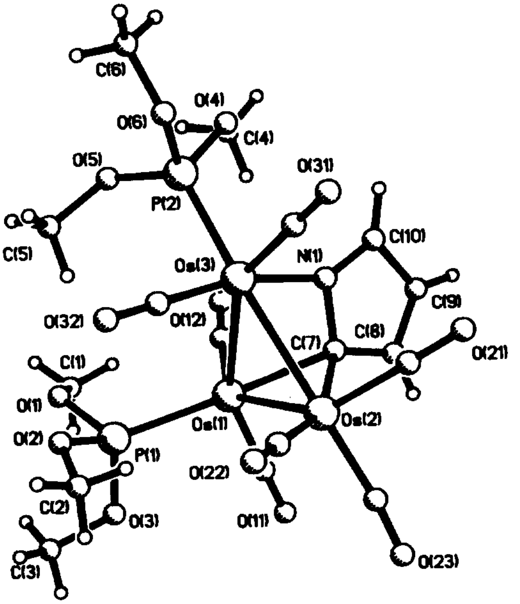

Fig. 9. Molecular structure of $Os_3(\mu\text{-}H)_2(CO)_7[P(OMe)_3]_2(C_4H_3N)$ (**24**) with atomic labelling. The two hydride ligands were not located directly and have been excluded from the diagram.

Table 2

Bond lengths (Å)

Os(1)-Os(2)	2.822(1)	Os(1)-Os(3)	3.020(1)
Os(1)-P(1)	2.301(4)	Os(1)-C(7)	2.180(16)
Os(1)-C(11)	1.892(14)	Os(1)-C(12)	1.893(16)
Os(2)-Os(3)	2.802(1)	Os(2)-C(7)	2.199(13)
Os(2)-C(21)	1.889(19)	Os(2)-C(22)	1.934(18)
Os(2)-C(23)	1.892(16)	Os(3)-P(2)	2.289(4)
Os(3)-N(1)	2.102(11)	Os(3)-C(31)	1.876(19)
Os(3)-C(32)	1.889(17)	P(1)-O(1)	1.592(13)
P(1)-O(2)	1.584(11)	P(1)-O(3)	1.580(12)
O(1)-C(1)	1.408(24)	O(2)-C(2)	1.417(23)
O(3)-C(3)	1.460(28)	P(2)-O(4)	1.591(13)
P(2)-O(5)	1.583(15)	P(2)-O(6)	1.591(11)
O(4)-C(4)	1.404(26)	O(5)-C(5)	1.432(23)
O(6)-C(6)	1.396(20)	N(1)-C(7)	1.401(17)
N(1)-C(10)	1.319(19)	C(7)-C(8)	1.435(20)
C(8)-C(9)	1.313(22)	C(9)-C(10)	1.457(22)
C(11)-O(11)	1.112(19)	C(12)-O(12)	1.142(20)
C(21)-O(21)	1.144(27)	C(22)-O(22)	1.114(23)
C(23)-O(23)	1.157(20)	C(31)-O(31)	1.138(24)
C(32)-O(32)	1.126(21)		

ing the *spiro*-carbon, C(7), may indicate some residual π-bonding to this atom suggesting that some aromatic character is retained by the ring in this bonding mode.

The observation of a phosphite or phosphine ligand occupying an axial position on a metal triangle is rare since both the steric and electronic factors would favour this type of bulky, π-acceptor ligand occupying an equatorial site. There is less steric crowding in equatorial sites, also, a good π-acceptor, such as a phosphite, would be able to attract more electron density to itself when *trans* to a metal–metal edge rather than when in competition for metal electron density with another good π-acceptor such as a *trans* axial carbonyl group [25]. However, in **24** one phosphite occupies an axial site, but, notably, is *trans* to the C(7) atom of the pyrrole ring rather than *trans* to a carbonyl. The structurally related cluster, $Os_3(\mu\text{-}H)(CO)_9$-

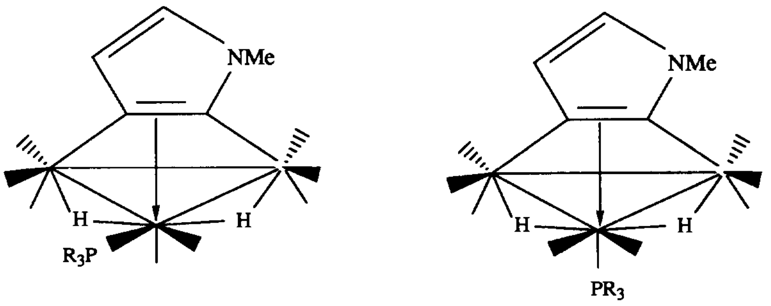

R = Et, **(26a)**
OMe, **(27a)**

R = Et, **(26b)**
OMe, **(27b)**

Fig. 10. Proposed structures of **26** and **27**.

Table 3

Bond angles (°)

Os(2)–Os(1)–Os(3)	57.2(1)	Os(2)–Os(1)–P(1)	122.9(1)
Os(3)–Os(1)–P(1)	109.4(1)	Os(2)–Os(1)–C(7)	50.2(4)
Os(3)–Os(1)–C(7)	62.7(4)	P(1)–Os(1)–C(7)	171.1(4)
Os(2)–Os(1)–C(11)	98.0(5)	Os(3)–Os(1)–C(11)	153.3(5)
P(1)–Os(1)–C(11)	92.0(6)	C(7)–Os(1)–C(11)	94.5(7)
Os(2)–Os(1)–C(12)	139.3(6)	Os(3)–Os(1)–C(12)	100.0(4)
P(1)–Os(1)–C(12)	95.5(6)	C(7)–Os(1)–C(12)	90.1(7)
C(11)–Os(1)–C(12)	93.4(6)	Os(1)–Os(2)–Os(3)	65.0(1)
Os(1)–Os(2)–C(7)	49.6(4)	Os(3)–Os(2)–C(7)	66.7(3)
Os(1)–Os(2)–C(21)	138.7(5)	Os(3)–Os(2)–C(21)	91.2(5)
C(7)–Os(2)–C(21)	90.9(6)	Os(1)–Os(2)–C(22)	119.2(6)
Os(3)–Os(2)–C(22)	92.1(5)	C(7)–Os(2)–C(22)	158.5(6)
C(21)–Os(2)–C(22)	93.5(8)	Os(1)–Os(2)–C(23)	102.0(6)
Os(3)–Os(2)–C(23)	165.2(6)	C(7)–Os(2)–C(23)	99.7(6)
C(21)–Os(2)–C(23)	95.1(7)	C(22)–Os(2)–C(23)	100.9(7)
Os(1)–Os(3)–Os(2)	57.8(1)	Os(1)–Os(3)–P(2)	111.4(1)
Os(2)–Os(3)–P(2)	165.7(1)	Os(1)–Os(3)–N(1)	66.9(3)
Os(2)–Os(3)–N(1)	70.0(3)	P(2)–Os(3)–N(1)	97.6(3)
Os(1)–Os(3)–C(31)	150.6(5)	Os(2)–Os(3)–C(31)	95.3(5)
P(2)–Os(3)–C(31)	92.7(5)	N(1)–Os(3)–C(31)	94.1(6)
Os(1)–Os(3)–C(32)	103.4(5)	Os(2)–Os(3)–C(32)	97.8(5)
P(2)–Os(3)–C(32)	93.9(5)	N(1)–Os(3)–C(32)	167.1(6)
C(31)–Os(3)–C(32)	91.1(8)	Os(1)–P(1)–O(1)	119.8(5)
Os(1)–P(1)–O(2)	120.2(5)	O(1)–P(1)–O(2)	92.9(6)
Os(1)–P(1)–O(3)	111.2(5)	O(1)–P(1)–O(3)	105.7(7)
O(2)–P(1)–O(3)	104.7(6)	P(1)–O(1)–C(1)	121.6(11)
P(1)–O(2)–C(2)	120.2(11)	P(1)–O(3)–C(3)	121.7(12)
Os(3)–P(2)–O(4)	118.5(5)	Os(3)–P(2)–O(5)	121.4(5)
O(4)–P(2)–O(5)	99.3(7)	Os(3)–P(2)–O(6)	110.1(5)
O(4)–P(2)–O(6)	99.2(7)	O(5)–P(2)–O(6)	105.4(8)
P(2)–O(4)–C(4)	125.9(13)	P(2)–O(5)–C(5)	122.3(12)
P(2)–O(6)–C(6)	122.5(12)	Os(3)–N(1)–C(7)	104.2(8)
Os(3)–N(1)–C(10)	146.4(9)	C(7)–N(1)–C(10)	109.2(11)
Os(1)–C(7)–Os(2)	80.2(5)	Os(1)–C(7)–N(1)	107.5(10)
Os(2)–C(7)–N(1)	103.6(9)	Os(1)–C(7)–C(8)	127.3(11)
Os(2)–C(7)–C(8)	127.0(11)	N(1)–C(7)–C(8)	107.2(11)
C(7)–C(8)–C(9)	106.9(13)	C(8)–C(9)–C(10)	109.5(13)
N(1)–C(10)–C(9)	107.1(12)	Os(1)–C(11)–O(11)	178.0(17)
Os(1)–C(12)–O(12)	174.3(17)	Os(2)–C(21)–O(21)	176.7(14)
Os(2)–C(22)–O(22)	176.5(20)	Os(2)–C(23)–O(23)	174.0(15)
Os(3)–C(31)–O(31)	177.3(16)	Os(3)–C(32)–O(32)	178.9(14)

(SPh)(PEt$_3$) [26], does show the presence of a phosphine in a *pseudo*-axial site. The presence of the axial phosphite in **24** adds weight to the spectroscopic assignment of axial phosphites and phosphines in complexes **13**–**20** alone.

(v) Reactions of $Os_3(\mu\text{-}H)_2(CO)_8(MeCN)(C_4H_2NMe)$ *(**8**) and* $Os_3(\mu\text{-}H)_2(CO)_7(MeCN)_2(C_4H_2NMe)$ *(**12**) with* PEt_3 *and* $P(OMe)_3$

The reaction of triethylphosphine or trimethylphosphite with $Os_3(\mu\text{-}H)_2(CO)_8(MeCN)(C_4H_2NMe)$ (**8**) yields two isomers in each case, **26a**, **26b** and **27a**, **27b**. The major isomers **26a** and **27a** have phosphine or phosphite ligand occupying an equatorial site with *trans* ^{31}P–^{1}H coupling to one hydride ligand (J(PH) = 23.4

Table 4

The IR and MS spectra of **13**–**29**

Compound	IR (ν(CO), cm^{-1} hexane)	MS (^{192}Os)
$Os_3(\mu\text{-}H)_2(CO)_8(PPh_3)(C_6H_4)$ (**13**) [a]	2080m, 2047s, 2039m, 2000s, 1976m.	1140
$Os_3(\mu\text{-}H)_2(CO)_8[(P(OMe)_3](C_6H_4)$ (**14**) [a]	2083m, 2048s, 2024w, 2001s, 1982w, 1969m.	1002
$Os_3(\mu\text{-}H)_2(CO)_7(PPh_3)_2(C_6H_4)$ (**15**) [a]	2063s, 2056s, 2046w, 2030s, 2002s, 1992s,sh, 1988s, 1978s, 1965s, 1940w, 1929w.	1374
$Os_3(\mu\text{-}H)_2(CO)_7[(P(OMe)_3]_2(C_6H_4)$ (**16**)	2082w, 2060m, 2038vs, 2011s, 1986s, 1960m.	1098
$Os_3(\mu\text{-}H)_2(CO)_8(PEt_3)(C_9H_6)$ (**17**)	2081m, 2047s, 2028s, 2002s, 1995s,sh, 1981w, 1966s.	1034
$Os_3(\mu\text{-}H)_2(CO)_8[P(OMe)_3](C_9H_6)$ (**18**)	2083m, 2048s, 2026w, 2004s,sh, 1983w, 1971m, 1959vw.	1040
$Os_3(\mu\text{-}H)_2(CO)_7(PEt_3)_2(C_9H_6)$ (**19**)	2082vvw, 2056w, 2043m, 2017s, 1998s, 1984mw, 1965s,sh, 1957s, 1946s, 1920vw.	1124
$Os_3(\mu\text{-}H)_2(CO)_7[P(OMe)_3]_2(C_9H_6)$ (**20**)	2062m, 2039vs, 2018s,sh, 2010vs, 1987vs, 1980s,sh, 1961m, 1952w.	1136
$Os_3(\mu\text{-}H)_2(CO)_8(PEt_3)(C_4H_3N)$ (**21**)	2082m, 2047vs, 2029vs, 2002s, 1986ms, 1974s, 1940vw.	985
$Os_3(\mu - H)_2(CO)_8[P(OMe)_3](C_4H_3N)$ (**22**)	2098w, 2082s, 2046vs,br, 2024w, 2000vs, 1990vs,br, 1970s, 1955w.	991
$Os_3(\mu\text{-}H)_2(CO)_7(PEt_3)_2(C_4H_3N)$ (**23**)	2054s, 2022vs, 1993s, 1976vs, 1962ms, 1954m, 1928m.	1075
$Os_3(\mu\text{-}H)_2(CO)_7[P(OMe)_3]_2(C_4H_3N)$ (**24**)	2060s, 2044s,br, 2006s, 1982vs, 1968m, 1948w.	1087
$Os_3(\mu\text{-}H)_2(CO)_7(MeCN)[P(OMe)_3](C_4H_3N)$ (**25**)	2059s, 2029vs, 2004m, 1980vs, 1968s, 1959m, 1945w.	parent peak not observed
$Os_3(\mu\text{-}H)_2(CO)_8(PEt_3)(C_4H_2NMe)$ (**26**)	2077m, 2043s, 2025s, 1994s, 1984ms, 1973w.	999
$Os_3(\mu\text{-}H)_2(CO)_8[P(OMe)_3](C_4H_2NMe)$ (**27**)	2098vw, 2079s, 2045vs,br, 1996vs,br, 1968s.	1005
$Os_39\mu\text{-}H)_2(CO)_7(PEt_3)_2(C_4H_2NMe)$ (**28**)	2051w, 2039w, 2014s, 1989s, 1977w, 1956ms, 1946m, 1928w.	1089
$Os_3(\mu\text{-}H)_2(CO)_7[P(OMe)_3]_2(C_4H_2NMe)$ (**29**)	2058m, 2037vs, 2003s, 1979vs, 1959m, 1943w.	1101

[a] Data obtained from ref. 10.

and 45.5 Hz, respectively) and *cis*-coupling to the other (J(PH) = 11.3 and 11.7 Hz, respectively), while the minor isomers **26b** and **27b** have the PR$_3$ ligand located mutually *cis* to two equivalent hydride ligands, in a manner similar to that in **14a** (Fig. 10).

The reactions of $Os_3(\mu\text{-}H)_2(CO)_7(MeCN)_2(C_4H_2NMe)$ (**12**) with PEt$_3$ and P(OMe)$_3$ in CH$_2$Cl$_2$ at room temperature produce the derivatives $Os_3(\mu\text{-}H)_2(CO)_7(PEt_3)_2(C_4H_2NMe)$ (**20**) and $Os_3(\mu\text{-}H)_2(CO)_7[P(OMe)_3]_2(C_4H_2NMe)$ (**29**). The ^{1}H NMR spectra of both **28** and **29** show the existence of three isomers in each case with the major one probably having a similar structure to those of **23** and **24**, i.e. both ligands being *cis* to the hydrides.

The spectroscopic data of clusters **13**–**29** are shown in Table 4 and Table 5.

Table 5

^{1}H NMR data of clusters **13–29**

Compound	^{1}H NMR[a] (δ, all *J* values in Hz)	
$Os_3(\mu\text{-}H)_2(CO)_8(PPh_3)(C_6H_4)$ (**13**)[b]	major isomer: 7.16–7.55 (m, 15H); 7.94 and 6.89 (AA′XX′, 4H); −18.09 (d, 2H, *J*(PH) = 9.2).	minor isomer: 7.10–7.55 (m, 1H); −16.14 (d, 1H, *J*(PH) = 24.2); −19.87 (d, 1H), *J*(PH) = 14.2). C_6H_4 signals broadened to baseline
$Os_3(\mu\text{-}H)_2(CO)_8[P(OMe)_3](C_6H_4)$ (**14**)[b]	major isomer: 7.82 (d, br, 2H); 6.77 (s, br, 2H); 3.34 (d, (H, *J*(PH) = 12.0); −16.85 (d, br, 1H); −20.95 (d, br, 1H). (203 K): −16.80 (d, 1H, *J*(PH) = 38.8); −21.18 (d, 1H, *J*(PH) = 14.5).	minor isomer: only $P(OMe)_3$ and hydride resonances identified 3.66 (s, br, 9H); −18.80 (s, br, 2H). (203 K): −18.91 (d, 2H, *J*(PH) = 10.9).
$Os_3(\mu\text{-}H)_2(CO)_7(PPh_3)_2(C_6H_4)$ (**15**)[b]	7.50 and 6.68 (AA′XX′, 4H); 7.0–7.5 (m, 30H); −17.20 (t, 1H, *J*(PH) = 8.8); −17.83 (d, 1H, *J*(PH) = 10.3).	
$Os_3(\mu\text{-}H)_2(CO)_7[(P(OMe)_3]_2(C_6H_4)$ (**16**)	7.77 and 6.70 (AA′XX′, 4H); 3.45 (br, s); −16.68 (br, s, 1H); −18.73 (br, s, 1H); −19.37 (br, s, 1H); −20.86 (br, s, 1H). (190 K):	
	major isomer: 7.76 (app. d, 1H, *J* = 8.0); 7.62 (app. d, 1H, *J* = 7.4); 6.78 (app. t, 1H, *J* = 7.3); 6.58 (app. t, 1H, *J* = 6.7); 3.25 (d, 9H, *J*(PH) = 12.4); 3.18 (d, (H, *J*(PH) = 11.3); −16.83 (dd, 1H, J_1 = 44.0, J_2 = 9.3); −21.33 (br, d, 1H, *J*(PH) = 14.8).	minor isomer: benzyne signals not resolved 3.66 (d, 9H, *J*(PH) = 12.1); 3.53 (d, 9H, *J*(PH) = 12.0); −16.69 (d, 1H, *J*(PH) = 15.0); −20.98 (d, 1H, *J*(PH) = 14.9).
$Os_3(\mu\text{-}H)_2(CO)_8(PEt_3)(C_9H_6)$ (**17**)	7.07–7.48 (m); 3.37 and 4.01 (AB quartet); 1.95 (m); 1.00 (m).	
	major isomer: −16.10 (d, 1H, *J*(PH) = 18.1); −21.03 (d, 1H, *J*(PH) = 11.9).	minor isomer: −16.20 (d, 1H, *J*(PH) = 18.7); −20.01 (d, 1H, *J*(PH) = 12.5).
$Os_3(\mu\text{-}H)_2(CO)_8[P(OMe)_3](C_9H_6)$ (**18**)	7.13–7.48 (m, 4H); 3.56 (d, 9H, *J*(PH) = 12.2); 3.13 (s, 2H); −16.94 (d, 1H, *J*(PH) = 37.8); −21.36 (d, 1H, *J*(PH) = 13.4).	
$Os_3(\mu\text{-}H)_2(CO)_7(PEt_3)_2(C_9H_6)$ (**19**)	7.01–7.33 (m, 4H); 3.94 and 3.65 (AB quartet, 2H); 2.11 (m, 12H); 1.29 (m, 18H); −15.68 (m, 1H); −20.49 (d, 1H), *J*(PH) = 13.7).	
$Os_3(\mu\text{-}H)_2(CO)_7[P(OMe)_3]_2(C_9H_6)$ (**20**)	7.01–7.45 (m, 4H); 3.54 (d, 9H, *J*(PH) = 11.5); 3.44 (d, 9H, *J*(PH) = 11.5); 3.08 (s, 2H); −16.75 (m, 1H); −21.22 (m, 1H).	
$Os_3(\mu\text{-}H)_2(CO)_8(PEt_3)(C_4H_3N)$ (**21**)	[c] 7.39 (br, s, 1H); 7.30 (d, 1H, *J* = 4.0); 6.52 (dd, 1H, J_1 = 4.0, J_2 = 0.8); 1.59 (m, 6H, *J*(PH) = 30.0); 1.00 (dt, 9H, *J*(PH) = 16.5); −14.68 (d, 1H), *J*(PH) = 22.0); −16.45 (d, 1H, *J*(PH) = 12.3).	
$Os_3(\mu\text{-}H)_2(CO)_8[P(OMe)_3](C_4H_3N)$ (**22**)	major isomer: 6.81 (d, 1H, *J* = 3.9); 6.76 (s, 1H); 5.87 (d, 1H, *J* = 4.0); 3.03 (d, 9H, *J*(PH) = 12.0); −16.05 (d, 1H, *J*(PH) = 51.3); −17.46 (d, 1H, *J*(PH) = 13.3).	minor isomer: 6.77 (d, 1H, *J* = 4.3); 6.67 (d, 1H, *J* = 3.6); 5.93 (d, 1H, *J* = 4.2); 2.84 (d, 9H, *J*(PH) = 11.8); −16.21 (d, 1H, *J*(PH) = 10.2); −17.89 (d, 1H, *J*(PH) = 12.0).

Table 5 (continued)

Compound	^{1}H NMR ^{a} (δ, all J values in Hz)	
$Os_3(\mu\text{-}H)_2(CO)_7(PEt_3)_2(C_4H_3N)$ **(23)**	7.42 (d, 1H, J = 4.1); 7.41 (br, s, 1H); 6.50 (dd, 1H, J_1 = 4.1, J_2 = 1.1); 2.00 (m, 12H); 1.13 (m, 18H); −15.63 (d, 1H, J(PH) = 11.6); −16.70 (dt, 1H, J(PH) = 9.9, J(HH) = 1.0).	
$Os_3(\mu\text{-}H)_2(CO)_7[P(OMe)_3]_2(C_4H_3N)$ **(24)**	7.44 (s, 1H); 7.42 (d, 1H, J = 3.9); 6.53 (d, 1H, J = 4.0); 3.69 (d, 9H, J(PH) = 12.0); 3.67 (d, 9H, J(PH) = 11.9); −15.73 (d, 1H, J(PH) = 10.5); −16.94 (d, 1H, J(PH) = 11.4).	
$Os_3(\mu\text{-}H)_2(CO)_7(MeCN)[P(OMe)_3]\text{-}(C_4H_3N)$ **(25)**	7.40 (s, 1H); 7.25 (d, 1H, J = 3.9); 6.38 (d, 1H, J = 4.2); 3.67 (d, 9H, J(PH) = 12.0); 2.52 (s, 3H); −14.27 (d, 1H, J(PH) = 3.0); −14.34 (d, 1H, J(PH) = 12.0).	
$Os_3(\mu\text{-}H)_2(CO)_8(PEt_3)(C_4H_2NMe)$ **(26)**	major isomer: 7.05 (d, 1H, J = 2.9); 6.59 (d, 1H, J = 2.9); 3.51 (s, 3H); 1.75 (m, 6H); 0.95 (dt, 9H); −15.73 (d, 1H, J(PH) = 23.4); −20.68 (d, 1H, J(PH) = 11.3).	minor isomer: 7.17 (d, 1H, J = 2.8); 6.76 (d, 1H, J = 2.8); 3.59 (s, 3H); 1.95 (m, 6H); 1.14 (dt, 9H); −18.68 (d, 2H, J(PH) = 10.3).
$Os_3(\mu\text{-}H)_2(CO)_8[P(OMe)_3]\text{-}(C_4H_2NMe)$ **(27)**	major isomer: 7.04 (d, 1H, J = 2.9); 6.60 (d, 1H, J = 2.9); 3.53 (s, 3H); 3.44 (d, 9H, J(PH) = 11.7); −16.98 (d, 1H, J(PH) = 45.5); −20.60 (d, br, 1H, J(PH) = 11).	minor isomer: 7.15 (d, 1H, J = 2.8); 6.74 (dd, 1H, J = 2.8, 1.6); 3.58 (s, 3H); 3.66 (d, 9H, J(PH) = 12.1); −18.07 (d, 2H, J(PH) = 11.0).
$Os_3(\mu\text{-}H)_2(CO)_7(PEt_3)_2(C_4H_2NMe)$ **(28)**	resonances for minor isomers not identified major isomer: ^{d} 7.02 (d, 1H, J = 2.8); 6.47 (d, 1H, J = 2.7); 3.48 (s, 3H); 1.90 (m, 12H); 0.93 (m, 18H); −17.38 (d, 1H, J(PH) = 10.5); −20.52 (d, 1H, J(PH) = 10.1).	
$Os_3(\mu\text{-}H)_2(CO)_7[P(OMe)_3]_2\text{-}(C_4H_2NMe)$ **(29)**	resonances for minor isomers not identified; major isomers: 7.04 (d, 1H, J = 2.8); 6.71 (dd, 1H, J_1 = 2.7, J_2 = 1.5); 3.63 (d, 9H, J(PH) = 12.0); 3.46 (d, 9H, J(PH) = 12.0); 3.55 (s, 3H); −17.79 (d, 1H, J(PH) = 10.2); −20.34 (d, 1H, J(PH) = 11.8).	

[a] Recorded in CD_2Cl_2 on a Bruker WM250 or WM400 spectrometer at room temperature, unless otherwise stated. [b] Data obtained from ref. 10. [c] Recorded in $CDCl_3$ solution. [d] Recorded in tetrachloroethane-d_2.

Experimental

The clusters $Os_3(\mu\text{-}H)_2(CO)_9(C_6H_4)$ (**1**), $Os_3(\mu\text{-}H)_2(CO)_9(C_9H_6)$ (**2**), $Os_3(\mu\text{-}H)_2(CO)_9(C_4H_3N)$ (**3**), and $Os_3(\mu\text{-}H)_2(CO)_9(C_4H_2NMe)$ (**4**) were prepared in the published methods [11,14–16].

(i) Activation of clusters $Os_3(\mu\text{-}H)_2(CO)_9Ar$ [Ar = C_6H_4 (1); C_9H_6 (2); C_4H_3N (3) and C_4H_2NMe (4)] with Me_3NO/MeCN

$Os_3(\mu\text{-}H)_2(CO)_9Ar$ (15 mg) was dissolved in freshly distilled acetonitrile (10 ml). To this solution was added dropwise an acetonitrile solution of Me_3NO (1 mole equiv.). The reaction mixture was stirred at r.t., and the reaction was followed by IR spectroscopy. The reaction was stopped after ca. 0.5 h, when all the starting material is consumed as shown by IR. The solvent was then removed *in vacuo* and $Os_3(\mu\text{-}H)_2(CO)_8(MeCN)Ar$ [Ar = C_6H_4 (**5**); C_9H_6 (**6**); C_4H_3N (**7**) and C_4H_2NMe (**8**)] thus obtained was used *in situ* for further reactions.

The same procedure was applied except that 2 mole equiv. of Me_3NO was used, and the bis-acetonitrile derivatives $Os_3(\mu\text{-}H)_2(CO)_7(MeCN)_2Ar$ [Ar = C_6H_4 (**9**); C_9H_6 (**10**); C_4H_3N (**11**) and C_4h_2NMe (**12**)] were obtained. These were also used *in situ* for further reactions.

(ii) Reactions of $Os_3(\mu\text{-}H)_2(CO)_8(MeCN)(C_6H_4)$ (5) with PR_3 (R = Ph, OMe)

Freshly made $Os_3(\mu\text{-}H)_2(CO)_8(MeCN)(C_6H_4)$ (**5**) (ca. 15 mg) was dissolved in CH_2Cl_2 (10 ml), to which an excess of PR_3 (R = Ph, OMe) was added. The reaction mixture was stirred at r.t. for 0.5 h (R = Ph) or 3 h (R = OMe). The solvent was then removed under reduced pressure, and the residue was chromatographed with 40% CH_2Cl_2 in hexane. $Os_3(\mu\text{-}H)_2(CO)_8(PPh_3)(C_6H_4)$ (**13**) was obtained in ca. 30% yield, together with two unidentified products ($m/e = 1662$, and 938, respectively). In the reaction with $P(OMe)_3$, $Os_3(\mu\text{-}H)_2(CO)_8[(P(OMe)_3](C_6H_4)$ (**14**) (ca. 60%) and $Os_3(\mu\text{-}H)_2(CO)_7[P(OMe)_3]_2(C_6H_4)$ (**16**) (ca. 10%) were isolated.

(iii) Reactions of $Os_3(\mu\text{-}H)_2(CO)_7(MeCN)_2(C_6H_4)$ (9) with PR_3 (R = Ph, OMe)

Freshly made $Os_3(\mu\text{-}H)_2(CO)_7(MeCN)_2(C_6H_4)$ (**9**) (ca. 15 mg) was dissolved in CH_2Cl_2 (10 ml), to which an excess of PR_3 (R = Ph, OMe) was added. The reaction mixture was stirred at r.t. for 0.5 h (R = Ph) or 2 h (R = OMe). The solvent was then removed under reduced pressure, and the residue was chromatographed with 50% CH_2Cl_2 in hexane. $Os_3(\mu\text{-}H)_2(CO)_7(PR_3)_2(C_6H_4)$ [R = Ph (**15**); OMe (**16**)] is produced in 60–70% yield.

(iv) Reactions of $Os_3(\mu\text{-}H)_2(CO)_8(MeCN)(C_9H_6)$ (6) with PR_3 (R = Et, OMe)

To a CH_2Cl_2 solution (10 ml) of freshly prepared $Os_3(\mu\text{-}H)_2(CO)_8(MeCN)(C_9H_6)$ (**6**) (15 mg) was added an excess of PR_3 (R = Et, OMe). The reaction mixture was stirred at r.t. for 24 h, and the solvent was then removed *in vacuo*. Work-up of the residue by TLC with 50% CH_2Cl_2 in hexane afforded $Os_3(\mu\text{-}H)_2(CO)_8(PR_3)(C_9H_6)$ in good yield [R = Et (**17**), 75%; R = OMe (**18**), 52%]. When R = OMe, the disubstituted derivative, $Os_3(\mu\text{-}H)_2(CO)_7[P(OMe)_3]_2(C_9H_6)$ (**20**) was also isolated in ca. 10% yield. The yield of **18** could be improved by reacting **6** with $P(OMe)_3$ in refluxing CH_2Cl_2 for 1.5 h.

(v) Reactions of $Os_3(\mu\text{-}H)_2(CO)_7(MeCN)_2(C_9H_6)$ (10) with PR_3 (R = Et, OMe)

To a CH_2Cl_2 solution (10 ml) of freshly prepared $Os_3(\mu\text{-}H)_2(CO)_7(MeCN)_2$-$(C_9H_6)$ (**10**) (15 mg) was added an excess of PR_3 (R = Et, OMe). The reaction mixture was stirred as r.t. for 22 h (R = Et) or 17.5 h (R = OMe). The solvent was then evacuated, and the residue worked up by TLC using 50% CH_2Cl_2 in hexane as eluent. $Os_3(\mu\text{-}H)_2(CO)_7(PR_3)_2(C_9H_6)$ was obtained as major product [R = Et (**19**), 60%; R = OMe (**20**), 68%], together with small amount of mono-substituted product, **17** or **18**, respectively. When the reaction of **10** with $P(OMe)_3$ was carried out in refluxing CH_2Cl_2, the same yield of **20** could be obtained with much shorter reaction time (1.5 h).

(vi) Reactions of $Os_3(\mu\text{-}H)_2(CO)_8(MeCN)(C_4H_3N)$ (7) with PR_3 (R = Et, OMe)

To a CH_2Cl_2 solution (10 ml) of freshly prepared $Os_3(\mu\text{-}H)_2(CO)_8(MeCN)$-

(C_4H_3N) (**7**) (15 mg) was added an excess of PR_3 (R = Et, OMe). The reaction mixture was stirred at r.t. for 3 h. The solvent was removed *in vacuo*, and the residue was worked up by TLC using 50% CH_2Cl_2 in hexane as eluent. The yellow compound $Os_3(\mu\text{-}H)_2(CO)_8(PR_3)(C_4H_3N)$ [R = Et (**21**), OMe (**22**)] was obtained in ca. 50% yield.

(vii) Reactions of $Os_3(\mu\text{-}H)_2(CO)_7(MeCN)_2(C_4H_3N)$ *(11) with* PR_3 *(R = Et, OMe)*

To a CH_2Cl_2 solution (10 ml) of freshly prepared $Os_3(\mu\text{-}H)_2(CO)_7(MeCN)_2$-$(C_4H_3N)$ (**11**) (15 mg) was added an excess of PR_3 (R = Et, OMe). The reaction mixture was stirred at r.t. for 1 h (R = Et) or 3 h (R = OMe). The solvent was removed *in vacuo*, and the residue was worked up by TLC using 50% CH_2Cl_2 in hexane as eluent. The yellow compounds $Os_3(\mu\text{-}H)_2(CO)_7(PEt_3)_2(C_4H_3N)$ (**23**) and $Os_3(\mu\text{-}H)_2(CO)_7[P(OMe)_3]_2(C_4H_3N)$ (**24**) were produced in 40 and 60% yield, respectively. In the reaction with $P(OMe)_3$, a second, yellow band was obtained and was characterised by spectroscopic data as $Os_3(\mu\text{-}H)_2(CO)_7[P(OMe)_3](MeCN)$-$(C_4H_3N)$ (**25**) (10%).

(viii) Reactions of $Os_3(\mu\text{-}H)_2(CO)_8(MeCN)(C_4H_2NMe)$ *(8) with* PR_3 *(R = Et, OMe)*

Freshly made $Os_3(\mu\text{-}H)_2(CO)_8(MeCN)(C_4H_2NMe)$ (**8**) (ca. 15 mg) was dissolved in CH_2Cl_2 (10 ml), to which an excess of PR_3 (R = Et, OMe) was added. The reaction mixture was stirred at r.t. for 1 h (R = Et) or 4 h (R = OMe). The solvent was then removed *in vacuo*, and the residue taken-up by CH_2Cl_2 was subjected to TLC using 50% CH_2Cl_2 in hexane as eluent. Apart from the small amount of unreacted starting material (**8**) recovered, the yellow compounds $Os_3(\mu\text{-}H)_2(CO)_8(PEt_3)(C_4H_2NMe)$ (**26**) and $Os_3(\mu\text{-}H)_2(CO)_8[P(OMe)_3](C_4H_2NMe)$ (**27**) were obtained in 60 and 50% yield, respectively.

(ix) Reactions of $Os_3(\mu\text{-}H)_2(CO)_8(MeCN)(C_4H_2NMe)$ *(12) with* PR_3 *(R = Et, OMe)*

Freshly prepared $Os_3(\mu\text{-}H)_2(CO)_7(MeCN)_2(C_4H_2NMe)$ (**12**) (ca. 15 mg) was dissolved in CH_2Cl_2 (10 ml), to which an excess of PR_3 (R = Et, OMe) was added. The reaction mixture was stirred at r.t. for 2.5 h (R = Et) or 2 h (R = OMe). The solvent was then removed *in vacuo*, and the residue taken-up by CH_2Cl_2 was subjected to TLC using 50% CH_2Cl_2 in hexane as eluent. Apart from the small amount of unreacted starting material (**12**) recovered, the yellow compounds $Os_3(\mu\text{-}H)_2(CO)_7(PEt_3)_2(C_4H_2NMe)$ (**28**) and $Os_3(\mu\text{-}H)_2(CO)_7[P(OMe)_3]_2(C_4H_2Me)$ (**29**) were obtained in 25 and 35% yield, respectively.

(x) Crystal structure determination for $H_2Os_3(CO)_7[P(OMe)_3]_2(C_4H_3N)$ *(24)*

Crystal data. $C_{17}H_{23}NO_{13}Os_3P_2$, M 1081.9, triclinic, a 9.519(3), b 10.165(3), c 14.942(4) Å, α 81.12(2), β 80.73(2), γ 80.50(3)°, V 1395.1(7) Å^3 (by least-squares refinement on diffractometer angles for 30 automatically centred reflections in the range $20 < 2\theta < 25°$, λ 0.71069 Å), space group $P\bar{1}$ (No. 2), $Z = 2$ $d = 2.575$ g cm^{-3}, $F(000)$ 988, yellow plate, crystal dimensions: $0.10 \times 0.35 \times 0.55$ mm, $\mu(\text{Mo-}K_\alpha)$ 138.19 cm^{-1}, μR 2.30.

Data collection and processing. Nicolet R3mV four-circle diffractometer, graphite monochromated Mo-K_α radiation, 96 step ω–2θ scans, scan range 1.40° plus K_α-separation, scan speed 3.0–29.3° mm^{-1}; 3942 reflections measured ($5 < 2\theta < 45°$, $+h$, $\pm k$, $\pm l$), 3562 unique [merging $R = 0.014$ on 380 equivalent reflections after empirical absorption correction (max., min. transmission factors = 0.675, 0.156)], giving 3194 reflections with $F > 4\sigma(F)$. No significant variation in intensities of three standard reflections.

Structure analysis and refinement. Direct methods (SHELXTL-PLUS: TREF) for Os atoms, followed by Fourier difference techniques for remaining non-hydrogen atoms. Full-matrix least-squares with all non-hydrogen atoms anisotropic. Methyl and aromatic H-atoms were placed in idealised positions and allowed to ride on the relevant C atom (C–H 0.96 Å); each type of H-atom was assigned a common isotropic thermal parameter which was refined. The hydrides were not located directly. The weighting scheme $w^{-1} = \sigma^2(F) + 0.002F^2$, with $\sigma(F)$ from counting statistics gave reasonable agreement analyses. Final, converged R and R_w values

Table 6

Atomic coordinates ($\times 10^4$) and equivalent isotropic displacement coefficients ($Å^2 \times 10^3$)

	x	y	z	U_{eq} [a]
Os(1)	864(1)	7557(1)	2401(1)	24(1)
Os(2)	2755(1)	9327(1)	2594(1)	28(1)
Os(3)	3955(1)	6608(1)	2688(1)	26(1)
P(1)	521(4)	7082(4)	1001(3)	32(1)
O(1)	207(12)	5625(11)	902(9)	51(5)
C(1)	−1041(24)	5120(18)	1368(16)	72(9)
O(2)	1805(12)	7053(11)	182(7)	45(4)
C(2)	2471(23)	8216(19)	−144(13)	64(8)
O(3)	−741(13)	8103(12)	605(8)	58(5)
C(3)	−1228(26)	7962(22)	−249(14)	79(10)
P(2)	4404(4)	4311(4)	2988(3)	36(1)
O(4)	4005(14)	3621(12)	4008(9)	60(5)
C(4)	2684(23)	3189(22)	4385(14)	75(9)
O(5)	3744(16)	3376(12)	2461(8)	59(5)
C(5)	3645(26)	3675(19)	1503(13)	71(9)
O(6)	6090(12)	3818(12)	2855(10)	65(6)
C(6)	6674(21)	2460(17)	2960(16)	68(8)
N(1)	2586(11)	6955(11)	3906(8)	28(4)
C(7)	1535(16)	8011(14)	3633(9)	31(5)
C(8)	629(16)	8382(15)	4446(11)	38(6)
C(9)	1108(19)	7569(17)	5138(11)	48(6)
C(10)	2359(17)	6653(16)	4803(10)	40(6)
C(11)	−865(17)	8781(14)	2493(12)	38(6)
O(11)	−1858(15)	9530(14)	2548(12)	80(6)
C(12)	−12(15)	6110(16)	3093(12)	42(6)
O(12)	−461(15)	5232(12)	3560(11)	72(6)
C(21)	3871(16)	9608(16)	3466(12)	43(6)
O(21)	4506(18)	9744(15)	4025(11)	85(7)
C(22)	4165(21)	9830(17)	1567(13)	51(7)
O(22)	5024(17)	10119(16)	1005(10)	84(7)
C(23)	1506(20)	10973(17)	2658(11)	43(6)
O(23)	716(14)	11968(12)	2622(10)	66(5)
C(31)	5617(18)	6825(15)	3142(13)	45(6)
O(31)	6647(13)	6975(15)	3383(10)	72(6)
C(32)	4951(17)	6661(17)	1486(12)	45(6)
O(32)	5527(15)	6688(15)	764(9)	69(6)

[a] Equivalent isotropic U defined as one third of the trace of the orthogonalized $U_{i/j}$ tensor.

are both 0.051. A final Fourier difference map showed ripples of ca. 2.0 e Å^{-3} close to the Os atom positions but no other regions of significant electron density. Final atomic coordinates are listed in Table 6. Copies of thermal parameter and structure factor tables may be obtained from the authors. Programs and computers used are given in reference 27.

Acknowledgements

We thank the Sino-British Friendship Scholarship Scheme for financial support (H.C.).

References

1 G.L. Gainsford, J.M. Guss, P.R. Ireland, R. Mason, C.W. Bradford and R.S. Nyholm, J. Organomet. Chem., 42 (1972) C70.

2 C.W. Bradford and R.S. Nyholm, J. Chem. Soc., Chem. Commun., (1972) 87.

3 A.J. Deeming, R.E. Kimber and M. Underhill, J. Chem. Soc., Dalton Trans., (1973) 2589.

4 M.I. Bruce, G. Shaw and F.G.A. Stone, J. Chem. Soc., Dalton Trans., (1972) 2094.

5 S.C. Brown, J. Evans and L.E. Smart, J. Chem. Soc., Chem. Commun., (1980) 1021.

6 A.J. Arce and A.J. Deeming, J. Chem. Soc., Dalton Trans., (1982) 1155.

7 A.J. Deeming, S.E. Kabir, N.I. Powell, P.A. Bates and M.B. Hursthouse, J. Chem. Soc., Dalton Trans., (1987) 1529.

8 W.R. Cullen, S.T. Chacon, M.I. Bruce, F.W.B. Einstein and R.H. Jones, Organometallics, 7 (1988) 2273.

9 A.J. Deeming and M. Underhill, J. Organomet. Chem., 42 (1972) C40.

10 (a) M.A. Gallop, PhD thesis, Cambridge, 1988; (b) M.A. Gallop, B.F.G. Johnson, J. Lewis, A. McCamley and R.N. Perutz, J. Chem. Soc., Chem. Commun., (1988) 1071.

11 R.J. Goudsmit, B.F.G. Johnson, J. Lewis, P.R. Raithby and M.J. Rosales, J. Chem. Soc., Dalton Trans., (1983) 2257.

12 P.R. Raithby and M.J. Rosales, Adv. Inorg. Chem. Radiochem., 29 (1985) 169.

13 D. Braga, F. Grepioni, A.D. Massey, B.F.G. Johnson and J. Lewis, J. Organomet. Chem., 369 (1989) C43.

14 A.J. Deeming, J. Organomet. Chem., 150 (1978) 123.

15 C.C. Yin and A.J. Deeming, J. Chem. Soc., Dalton Trans., (1982) 2563.

16 A.J. Arce, Y. De Sanctis and A.J. Deeming, J. Organomet. Chem., 311 (1986) 371.

17 A.J. Deeming, R.S. Nyholm and M. Underhill, J. Chem. Soc., Chem. Commun., (1972) 224.

18 A.J. Deeming, I.P. Powell, M.B. Hursthouse and J.D.J. Backer-Dirks, J. Chem. Soc., Dalton Trans., (1981) 1879.

19 K.-J. Kneuper and J.R. Shapley, Organomet. 6 (1987) 2455.

20 A.J. Deeming, J.E. Marshall, D. Nuel, G. O'Brien and N.I. Powell, J. Organomet. Chem., 384 (1990) 347.

21 H. Chen, B.F.G. Johnson, J. Lewis and P.R. Raithby, J. Organomet. Chem., 376 (1989) C7.

22 H. Chen, B.F.G. Johnson and J. Lewis, Organometallics, 8 (1989) 2965.

23 M.W. Day, K.I. Hardcastle, A.J. Deeming, A.J. Arce and Y. De Sanctis, Organometallics, 9 (1990) 6.

24 A.G. Orpen, J. Chem. Soc., Dalton Trans., (1980) 2509.

25 E.J. Ditzel, B.E. Hanson, B.F.G. Johnson and J. Lewis, J. Chem. Soc., Dalton Trans., (1987) 1285.

26 E.J. Ditzel, M.P. Gomez-Sal, B.F.G. Johnson, J. Lewis and P.R. Raithby, J. Chem. Soc., Dalton Trans., (1987) 1623.

27 SHELXTL PLUS, Release 3.4, Nicolet Instruments Corp., USA, 1988.